Available online at www.sciencedirect.com
ScienceDirect
Progress in Natural Science 18 (2008) 729–733
Progress in Natural Science
www.elsevier.com/locate/pnsc

CFD simulation of fluidization quality in the three-dimensional fluidized bed

Kai Zhang [a,*], Stefano Brandani [b], Jicheng Bi [c], Jianchun Jiang [d]

[a] State Key Lab of Heavy Oil Processing, China University of Petroleum, Beijing 102249, China
[b] IMP-SEE, University of Edinburgh, The King's Buildings, Edinburgh EH9 3JL, UK
[c] State Key Lab of Coal Conversion, Institute of Coal Chemistry, Chinese Academy of Sciences, Taiyuan 030001, China
[d] Institute of Chemical Industry of Forest Products, Chinese Academy of Forestry, Nanjing 210042, China

Received 7 January 2008; received in revised form 2 February 2008; accepted 2 February 2008

Abstract

Multiphase computational fluid dynamics (CFD) has become an alternative method to experimental investigation for predicting the fluid dynamics in gas–solid fluidized beds. The model of Brandani and Zhang, which contains additional terms in both the gas- and solid-phase momentum equations, is employed to explore homogeneous fluidization of Geldart type A particles and bubbling fluidization of Geldart type B particles in three-dimensional gas-fluidized beds. In this model, only a correlation for drag force is necessary to close the governing equations. Two kinds of solids, i.e., fine alumina powder ($d_p = 60$ μm and $\rho_p = 1500$ kg/m^3) and sand ($d_p = 610$ μm and $\rho_p = 2500$ kg/m^3), are numerically simulated in a rectangular duct of 0.2 m (long) × 0.2 m (wide) × 0.5 m (high) size. The results show good agreement with the classic theory of Geldart.

Keywords: Three-dimensional gas–solid fluidized bed; Fluidization quality; CFD simulation

1. Introduction

Gas–solid fluidized beds are extensively applied in the process industry because of their advantageous properties including isothermal conditions throughout the bed, excellent heat and mass transfer and the possibility of continuous operation. These applications cover a wide range of physical and chemical processes, such as fluidized bed granulation, catalytic cracking of oil, and combustion of coal. In order to obtain the desired product specifications, maximize efficiency and enhance safety, it is meaningful to select an appropriate gas–solid contacting mode in the fluidized beds. In general, fluidization can be divided simply into two classes: homogeneous fluidization and bubbling fluidization [1]. The homogeneous fluidization appears in liquid–solid systems and gas–solid systems of Geldart A particles [2] when the superficial gas velocity ranges from the minimum fluidization velocity to the minimum bubbling velocity. Its characteristic is that particles are distributed uniformly in the fluid, and bubbles and agglomerates do not form. On the other hand, bubbling fluidization appears in gas–solid systems when the superficial gas velocity is greater than the minimum bubbling velocity. Its characteristic is that particle distribution in the gas is not uniform, namely there are gas bubbles with very low solids' content and a separate dense particle phase.

Computational fluid dynamics (CFD) is becoming an emerging method to explore the complicated fluid dynamics in gas–solid fluidized bed since Davidson first analyzed single-bubble motion in an infinite fluidized bed. These CFD models are commonly divided into Eulerian–Lagrangian and Eulerian–Eulerian approaches. The former considers the solid phase at a particle level, whilst the latter treats

* Corresponding author. Tel.: +86 10 89733939; fax: +86 10 69724721.
E-mail address: kaizhang@cup.edu.cn (K. Zhang).

1002-0071/$ - see front matter © 2008 National Natural Science Foundation of China and Chinese Academy of Sciences. Published by Elsevier Limited and Science in China Press. All rights reserved.
doi:10.1016/j.pnsc.2008.02.002

both gas and solid phases as interpenetrating continuous media. The bubbling fluidization, especially for Geldart B particles [2], was extensively investigated using either Eulerian–Lagrangian or Eulerian–Eulerian CFD models in the past 30 years [3–8]. Most of Eulerian–Lagrangian simulations for homogeneous fluidization were conducted in two-dimensional beds [9–13] due to the lack of computer resources and complexity of the theoretical models. A case study was carried out by Ye et al. [12], who investigated the effect of particle and gas properties on the fluidization quality. However, their calculations were carried out with 36,000 particles, and adopted time steps in the order of 10^{-5} and 10^{-6} s for gas and solid phases, respectively. It is clear that the Eulerian–Lagrangian method is computationally too intensive to apply at an engineering scale, even in the near feature [8]. van Wachem et al. [7] suggested that the Eulerian–Eulerian method was a feasible approach for performing parametric investigations and scale-up and design studies in fluidized beds. Notwithstanding the intense numerical research that has been conducted, there is still no consensus on solid-phase viscosity, solid stress modulus, and restitution coefficient [8].

Based on the two-fluid theory, we proposed a mathematical model by introducing additional terms into both gas- and solid-phase momentum balance equations, and two-dimensional simulations concerning the homogeneous fluidization of Geldart A particles and the bubbling and jetting fluidization of Geldart B particles have been accomplished in the platform of CFX 4.4 by adding the user-defined Fortran subroutines [8,14]. The aim of this study is to simulate the fluidization quality in a three-dimensional bed using the model of Brandani and Zhang [14].

2. Hydrodynamic model and numerical procedure

2.1. Hydrodynamic model

The hydrodynamic model is based upon the one-dimensional equations where gas phase is considered inviscid. In principle, three kinds of additional forces have to be considered in the momentum balance equations for particle suspension: forces resulting from interactions between the fluid and solid particles; forces from direct particle–particle interactions; forces from averaging procedures of body forces needed to obtain continuum formulations. Particle–particle interactions are obviously dominant when the velocity of the gas is less than the minimum fluidization velocity, since the momentum balance equations cannot describe a fixed bed in the absence of these terms. However, once the bed is fluidized the overall effect of particle–particle contacts over the entire bed can be negligible. Therefore, a two-fluid model considering the effect of the discrete nature of the particles on both the gas and particle phases was proposed by introducing additional forces in fluid and solid momentum balance equations [14]. The control equations for describing gas and solid flows in the three-dimensional cold model of fluidized beds are given below:

Continuity equations:

Gas phase

$$\frac{\partial \varepsilon_g}{\partial t} + \nabla \cdot (\varepsilon_g \boldsymbol{u_g}) = 0 \tag{1}$$

Particle phase

$$\frac{\partial \varepsilon_p}{\partial t} + \nabla \cdot (\varepsilon_p \boldsymbol{u_p}) = 0 \tag{2}$$

Momentum equations:

Gas phase

$$\frac{\partial (\varepsilon_g \rho_g \boldsymbol{u_g})}{\partial t} + \nabla \cdot (\varepsilon_g \rho_g \boldsymbol{u_g} \boldsymbol{u_g}) = \boldsymbol{F_g} \tag{3}$$

Particle phase

$$\frac{\partial (\varepsilon_p \rho_p \boldsymbol{u_p})}{\partial t} + \nabla \cdot (\varepsilon_p \rho_p \boldsymbol{u_p} \boldsymbol{u_p}) = \boldsymbol{F_s} \tag{4}$$

where ε represents the volume fraction ($\varepsilon_g + \varepsilon_p = 1$), F the net force per unit volume and ρ the density. The subscripts g and p indicate gas and particle phase, respectively. In order to close the governing equations, the net primary force, F, needs to be derived from the above basic variables.

Particle-phase force components are the following:

In the horizontal direction

$$F_{px} = C_D \frac{3\varepsilon_p \rho_g (u_g - u_p) \cdot \left|(\boldsymbol{u_g} - \boldsymbol{u_p})\right|}{4 d_p} \varepsilon_g^{-1.8} - \varepsilon_p \frac{\partial p}{\partial x} \tag{5}$$

In the lateral direction

$$F_{py} = C_D \frac{3\varepsilon_p \rho_g (v_g - v_p) \cdot \left|(\boldsymbol{u_g} - \boldsymbol{u_p})\right|}{4 d_p} \varepsilon_g^{-1.8} - \varepsilon_p \frac{\partial p}{\partial y} \tag{6}$$

In the vertical direction

$$F_{pz} = C_D \frac{3\varepsilon_p \rho_g (w_g - w_p) \cdot \left|(\boldsymbol{u_g} - \boldsymbol{u_p})\right|}{4 d_p} \varepsilon_g^{-1.8} + \varepsilon_p \rho_p g - \varepsilon_p \frac{\partial p}{\partial z} - d_p [2\varepsilon_p \rho_p + (1 - 2\varepsilon_p)\rho_g] g \frac{\partial \varepsilon_p}{\partial z} \tag{7}$$

Gas-phase force components are the following:

In the horizontal direction

$$F_{gx} = -C_D \frac{3\varepsilon_p \rho_g (u_g - u_p) \cdot \left|(\boldsymbol{u_g} - \boldsymbol{u_p})\right|}{4 d_p} \varepsilon_g^{-1.8} - \varepsilon_g \frac{\partial p}{\partial x} \tag{8}$$

In the lateral direction

$$F_{gy} = -C_D \frac{3\varepsilon_p \rho_g (v_g - v_p) \cdot \left|(\boldsymbol{u_g} - \boldsymbol{u_p})\right|}{4 d_p} \varepsilon_g^{-1.8} - \varepsilon_g \frac{\partial p}{\partial y} \tag{9}$$

In the vertical direction

$$F_{gz} = -C_D \frac{3\varepsilon_p \rho_g (w_g - w_p) \cdot \left|(\boldsymbol{u_g} - \boldsymbol{u_p})\right|}{4 d_p} \varepsilon_g^{-1.8} + \varepsilon_g \rho_g g - \varepsilon_g \frac{\partial p}{\partial z} - d_p [(1 - 2\varepsilon_g)\rho_p + 2\varepsilon_g \rho_g] g \frac{\partial \varepsilon_g}{\partial z} \tag{10}$$

The terms on the right side of Eqs. (7) and (10) are interphase drag, gravity, pressure drop, and the additional force. The empirical Dallavalle relation [15] is used to express the drag coefficient C_D:

$$C_D = \left(0.63 + \frac{4.8}{\sqrt{Re}}\right)^2 \tag{11}$$

where

$$Re = \frac{\varepsilon_g \rho_g |\boldsymbol{u}_g - \boldsymbol{u}_p| d_p}{\mu_g} \tag{12}$$

2.2. Numerical method

A finite volume method is used to solve numerically the set of partial differential equations (1)–(4) based on conservation principles. The simulations are conducted with the commercial CFD code CFX 4.4. All terms in the governing equations are discretized in space using the second-order centered differencing apart from the advection terms, which are obtained using the Rhie–Chow interpolation formula. The Rhie–Chow algorithm [16] is an effective method to prevent chequerboard oscillations of pressure on the co-located grid regarding the velocity–pressure coupling relation. As the default option of CFX 4.4, a fully implicit backward difference time stepping procedure has been implemented. Different differencing methods are used to treat the advection terms: central differencing scheme for gas or solid volume fraction, upwind differencing scheme for the shared pressure field, and hybrid differencing scheme for all velocity components. To resolve the algebraic equations derived by integrating transport equations over control volumes, iteration is used at two levels in CFX 4.4. An inner iteration solves for the spatial coupling for each variable and an outer iteration for the coupling between variables. However, the treatment of pressure is slightly different from the above description. The SIMPLEC algorithm, an extension of the semi-implicit method for pressure-linked equations (SIMPLE) algorithm, is implemented to deal with the velocity–pressure coupling. Under-relaxation factors in the outer iteration are 0.65 for all variables except pressure for which it is set as 1.0. The linear equation for each variable is solved by Block Stone's method in the inner iteration.

2.3. Simulation procedure

A three-dimensional fluidized bed of 0.2 m (long) × 0.2 m (wide) × 0.5 m (high) size is simulated in this study. Fine alumina and sand are used as solid particles, whose physical properties are listed in Table 1. The uniform staggered grid is 40 (long) × 40 (wide) × 100 (high) size. The solid particles are fluidized by air at ambient conditions. Time step is selected as 10^{-4} s. Initial bed heights are 0.3 m and 0.25 m for alumina and sand particles, respectively.

The Dirichlet boundary condition is used at the inlet, i.e., a uniform gas inlet velocity is specified at the bottom of the bed. Pressure boundary serves as the outlet of the freeboard, where a constant pressure (atmospheric) is set. All walls are treated using the no slip boundary conditions for both gas and particle phases.

Table 1
Physical properties of solid particles

Solid	d_p (m)	ρ_p (kg/m^3)	u_{mf} (m/s)	Geldart classification
Alumina	60×10^{-6}	1550	0.00354	Group A
Sand	610×10^{-6}	2500	0.446	Group B

Initially, the lower part of the fluidized bed is filled randomly with particles at the minimum fluidization state. The upper part of the fluidized bed is freeboard, which makes sure that particle concentration at the top of the bed is negligible. In the freeboard, the solid volume fraction is zero. However, this can result in unrealistic values for the particle-velocity field and poor convergence. For this reason, a solid volume fraction of 10^{-10} is set in the freeboard. It is essential that a very small number of particles filled within the whole freeboard can provide more realistic results for the particle velocity in this region, but without any influence on the fluid dynamics in the fluidized bed. Axial gas velocity corresponds to the minimum fluidization velocity, whilst horizontal and lateral gas velocities and the particle phase velocity vector are 0. The pressure profile in the whole bed is calculated from the hydrostatic bed height.

3. Results and discussion

3.1. Homogeneous fluidization for Geldart A particles

This model is extended to a three-dimensional geometry. Accordingly, an attempt is made to explore the minimum fluidization state. Given the increase in computational time in the three-dimensional bed in comparison to the two-dimensional one, this simulation is limited to 1.0 s. Results show that the local solid volume fraction within the bed keeps the initial solid volume fraction (0.45), and the bed height is 0.3 m throughout the simulation period. It is well known that the bed pressure drop is one of the most important macroscopic parameters to characterize the gas–solid fluidization. By combining the gas and solid momentum equations (3) and (4) the mixture momentum balance becomes

$$\frac{\partial(\varepsilon_p \rho_p \boldsymbol{u}_p)}{\partial t} + \frac{\partial(\varepsilon_g \rho_g \boldsymbol{u}_g)}{\partial t} + \nabla \cdot (\varepsilon_p \rho_p \boldsymbol{u}_p \boldsymbol{u}_p) + \nabla \cdot (\varepsilon_g \rho_g \boldsymbol{u}_g \boldsymbol{u}_g) = F_p + F_g \tag{13}$$

Substituting Eqs. (7) and (10) into Eq. (13), and neglecting acceleration and additional forces, the one-dimensional formulation in the vertical direction is obtained.

$$-\frac{dp}{dz} = (\varepsilon_g \rho_g + \varepsilon_p \rho_p) g \tag{14}$$

Therefore, a common formula for the total bed pressure drop is given as follows:

$$-\Delta P = (\varepsilon_g \rho_g + \varepsilon_p \rho_p) g \Delta h \quad (15)$$

As expected, simulated bed pressure drop is in good agreement with its calculated value by Eq. (15), which indicates that the drag force acting on all particles is equal to the gravitational force holding the solid within the fluidized bed.

In gas–solid fluidized beds, Geldart A particles present an interval of non-bubbling expansion (homogeneous fluidization) between the minimum fluidization velocity and the minimum bubbling velocity. The homogeneous expansion is technologically the most attractive of the processes when uniform conditions are desirable because gas bypassing and solid-phase dead zone are carefully avoided and each particle is used efficiently. To test the predictive capability for homogeneous fluidization, three half-round columns with a diameter of 0.05 m, where the solid volume fraction is 10^{-10}, at the base of the bed are arranged when time is zero. Fig. 1 shows the evolution of these finite perturbations within the bed, where the iso-surface of solid volume fraction is 0.52. Similar to the computational results in the two-dimensional fluidized bed [8,14], these small voids first become large, then leave the interface between the dense phase and the freeboard. Finally, the whole bed returns to the homogeneous fluidization state.

3.2. Bubbling fluidization for Geldart B particles

In the gas–solid fluidized bed of Geldart B particles, bubbles appear at or only slightly above the minimum fluidization velocity. The conversion in the fluidized bed reactor depends upon the extent of heat and mass transfer, which are strongly influenced by the mixing action of bubbles and other non-homogeneities associated with the unstable fluidized state. Since the model does not include particle–particle forces, for Geldart B powders the resulting simulations may include solid volume fractions, which exceed the physical limits corresponding to a fixed bed. To deal with this problem, several researchers added a solid-phase pressure term in the solid momentum equations [8]. According to Gidaspow, this term is of numerical significance only when the void fractions go below the minimum fluidization void fraction. It also helps to make the system numerically stable, because it converts the imaginary characteristics into real values. For some calculations, it is necessary to adjust this stress to prevent the void fraction from reaching impossibly low values [5]. However, Massoudi et al. [17] compared nine empirical relations for the modulus of elasticity. They calculated two formulations under the same condition and found that the results (-84.3 and -5.06×10^6 N/m^2) were orders of magnitude apart. The additional solid-phase pressure can prevent solid concentration exceeding the maximum value, but the parameters in this term depend strongly upon the gas–solid system. On the other hand, a different method proposed by Chen et al. [1,18] was to add a particle pressure force term to the particle phase momentum equations when solid concentration was greater than its upper limitation. This method is based on a point relaxation technique without linearization, and the particle pressure adjustment is performed on a single-grid-point basis. Unfortunately, the approach by Chen et al. [1,18] cannot be used directly in CFX 4.4. Accordingly, we suggested a similar method, which is to couple a rebuilt of excess solid concentration with a correction of the corresponding momentum equations in an intermediate step [8,14].

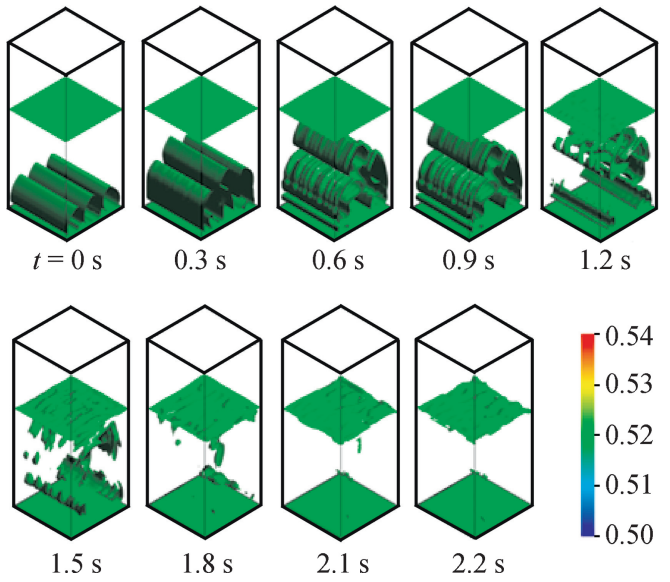

Fig. 1. Evaluation of the homogeneous fluidization (with initial small void perturbation).

During the numerical computation, it is important to determine the void boundary. Gidaspow et al. [3] defined the contour line of the solid volume fraction as 0.20, whilst Kuipers et al. [4] chose it as 0.15. Fig. 2 shows a series of snapshots of the iso-surface of solid volume fraction being 0.20. Similar to the simulation in the two-dimensional fluidized bed [8,14], the bed homogeneously expands in the beginning period (0.20 s or so). Then, some voids (or perturbations) randomly appear within the bed, which results in a bubbling fluidization state. Once bubbles detach from the interface between the dense phase and freeboard, the fluctuation of the interface becomes weak, and a stable bubbling fluidization has formed, accompanied by random coalescence or break-up of bubbles. This phenomenon indicates that the whole process can be divided into start-up and quasi-steady bubbling fluidization stages.

4. Conclusions

The performance of a gas–solid fluidized bed greatly depends on the hydrodynamic behavior of the system. Reliable design of commercial-scaled installments requires not only detailed understanding of the highly complex flow phenomena but also detailed knowledge of how the hydrodynamics are affected by both geometry and unit scale-up. The prediction of fluidization quality has been at the center of many years of experimental research and numerical

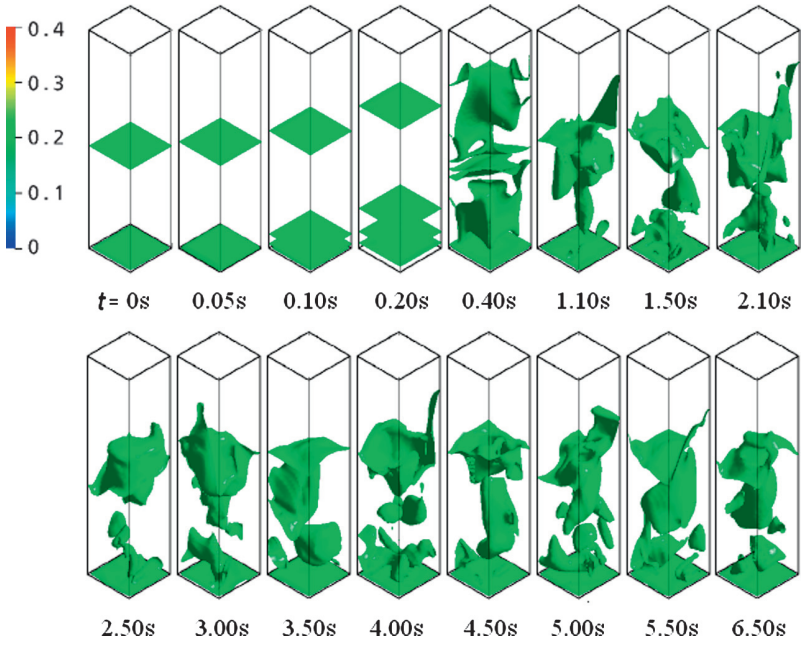

Fig. 2. Evaluation of the bubbling fluidization ($u_g = 2u_{mf}$).

computation. The ability to predict homogeneous or bubbling fluidization is needed to decide which configuration to choose depending on the features of the process to be carried out in the fluidized bed.

A recently developed mathematical model based on the two-fluid theory is adapted to simulate both homogeneous fluidization of Geldart A particles and bubbling fluidization of Geldart B particles in a three-dimensional gas–solid fluidized bed. The numerical results show good agreement with the classic theory of Geldart. This model is straightforward to use since it does not include adjustable parameters and has the capability to predict the fluidization behavior with similar results to the more complex Eulerian–Eulerian models based on the kinetic theory of granular flow.

Acknowledgements

Financial support from National Key Technology R&D Program of China (2006BAD07A0301), National Natural Science Foundation of China (20476057 and 20490200), and Key Laboratory of Coal Conversion (04-202) is gratefully acknowledged.

References

[1] Gibilaro L. Fluidization dynamics. London: Butterworth Heinemann; 2001.
[2] Geldart D. Types of fluidization. Powder Tech 1973;7(5):285–92.
[3] Gidaspow D, Ettehadleh B. Fluidization in two-dimensional beds with a jet. II. Hydrodynamic modeling. I&EC Fundam 1982;22(2):193–201.
[4] Kuipers JAM, Tammes H, Prins W, et al. Experimental and theoretical porosity profiles in two-dimensional gas-fluidized bed with a central jet. Powder Tech 1992;71(1):87–93.
[5] Gidaspow D. Multiphase flow and fluidization – continuum and kinetic theory descriptions. New York: Academic Press; 1994.
[6] Arastoopour H. Numerical simulation and experimental analysis of gas/solid flow systems: 1999 Fluor-Daniel Plenary lecture. Powder Tech 2001;119(2–3):59–67.
[7] van Wachem BGM, Schouten JG, van den Bleek CM, et al. Comparative analysis of CFD models of dense gas–solid system. AIChE J 2001;47(5):1035–51.
[8] Zhang K, Brandani S, Bi J. Computational fluid dynamics for dense gas–solid fluidized beds. Progr Nat Sci 2005;15:42–51, [special issue].
[9] Xu BH, Zhou YC, Yu AB, et al. Force structures in gas fluidized beds of fine powders. In: Proceedings of World Congress on particle technology 4 (CD-ROM), Sydney, Australia, July 21–25, 2002. p. 331.
[10] Ye M, van der Hoef MA, Kuipers JAM. A numerical study of fluidization behavior of Geldart A particles using a discrete particle model. Powder Tech 2004;139(2):129–39.
[11] Ye M, van der Hoef MA, Kuipers JAM. Discrete particle simulation of the homogeneous fluidization of Geldart A particles. In: Fluidization, vol. XI: Present and future for fluidization engineering. New York: Engineering Foundation; 2004. p. 699–706.
[12] Ye M, van der Hoef MA, Kuipers JAM. The effects of particle and gas properties on the fluidization of Geldart A particles. Chem Eng Sci 2005;60(16):4567–80.
[13] Di Renzo A, Di Maio FP. Homogeneous and bubbling fluidization regimes in DEM–CFD simulations: hydrodynamic stability of gas and liquid fluidized beds. Chem Eng Sci 2007;62(1–2):116–30.
[14] Brandani S, Zhang K. A new model for the prediction of the behaviour of fluidized beds. Powder Tech 2006;163(1–2):80–7.
[15] Dallavalle JM. Micromeritics. 2nd ed. London: Pitman; 1948.
[16] Rhie CM, Chow WL. Numerical study of the turbulent flow past an airfoil with trailing edge separation. AIAA J 1983;21(11):1527–32.
[17] Massoudi M, Rajagopal KR, Ekmann JM, et al. Remarks on the modeling of fluidized systems. AIChE J 1992;38(3):471–2.
[18] Chen Z, Gibilaro LG, Jand N. Particle packing constraints in fluid–particle system simulation. Comput Chem Eng 2003;27(3):681–7.